



## How Aeolian Dust Deteriorate Ambient Particulate Air Quality along an Expansive River Valley in Southern Taiwan? A Case Study of Typhoon Dokuri

Chun-Chung Lu, Chung-Shin Yuan\*, Tsung-Chang Li

*Institute of Environmental Engineering, National Sun Yat-Sen University, Kaohsiung 80424, Taiwan*

### ABSTRACT

Aeolian dust episodes (ADEs) frequently occurred at the bare lands of the riverbeds in Kaoping River are emerging disasters in Southern Taiwan in the past few years. However, their influences on ambient particulate air quality due to the outflow circulation of typhoons have not been addressed in such a subtropical region. This study aims to investigate the association between typhoons and ADEs and their influences on the ambient particulate air quality, which might occur in East Asia. Four sites along the Kaoping River were selected to collect PM<sub>10</sub> with high-volume samplers during and after the ADE accompanying with Typhoon Dokuri on June 29, 2012. During the ADE, PM<sub>10</sub> concentration rose as high as 30–40 folds higher than those on regular days. Chemical composition of PM<sub>10</sub> was further analyzed to verify several valuable indicators including the molar ratios of [Cl<sup>-</sup>]/[Na<sup>+</sup>] (0.95–1.02), the mass ratios of Fe/Cd (211.6–3957), and the mass ratios of OC/EC (1.18–1.35). Nevertheless, the chloride deficit phenomenon was not favorable during the ADE. Moreover, CMB receptor modeling results showed that aeolian dust and sea-salts were major contributors of PM<sub>10</sub> during the ADE. Along the Kaoping River, the contribution of aeolian dust to PM<sub>10</sub> ranged from 11.5 to 33.1% during the ADE, and reduced to 7.2–23.0% after the ADE. However, a small amount of finer aeolian dust could be still suspended in the ambient air after the ADE. Moreover, integrating SURFER software and WRF model was appropriate to locate the hot spots influenced by the ADE.

**Keywords:** Aeolian dust episodes (ADEs); Typhoon outflow circulation; Particulate air quality; Chemical characteristics; Source apportionment.

### INTRODUCTION

Aeolian dust is one of the vital sources of suspended particulate matter (PM) in ambient air nearby dry bare lands or fluvial basin areas. Aeolian dust triggered by specific weather conditions of particular landscapes have been emphasized worldwide (Chow *et al.*, 2003; Mkoma *et al.*, 2009; Wang *et al.*, 2015). South African study has focused on two large pan complexes in northern Namibia (Bryant *et al.*, 2007). A researcher captured the image of dust fugitively emitted from the dry ephemeral river valleys along the Namibian coast by adopting photography and imagery skills (Eckardt *et al.*, 2005). Other researchers found that the total suspended particulate emissions from dry land basins were highly related to several affecting factors (e.g., air temperature, soil silt content, and wind speed) (Lin *et al.*, 2007; Chang *et al.*, 2011; Syu *et al.*, 2016). Taiwan Environmental Protection Administration (TEPA) reported

that aeolian dust were the dominant air pollutants in the estuaries of major rivers of central Taiwan in winter (Taiwan EPA, 2009). The findings of previous studies related to aeolian dust from all over the world, their causes, contributing factors, characteristics, and influences have exhibited obvious differences. Although ADEs are becoming a substantial concern of general public and local environmental agencies, they have not been adequately investigated in Taiwan and over the world.

The TEPA reported that ADEs observed in central Taiwan solely occurred in the periods of northeastern Monsoons. An occasional pattern of poor ambient particulate air quality has frequently been recorded during the drought season in recent years (Lin *et al.*, 2007; Taiwan EPA, 2009; Kuo *et al.*, 2010; Syu *et al.*, 2016). However, ADEs that occurred exhibited distinct characteristics with specific weather conditions in southern Taiwan during the typhoon seasons (May–October). The features of ADEs observed in the Kaoping River Valley are distinct from those in central Taiwan. Most rivers in Taiwan flow westward or eastward since the Central Mountain Range with the peak heights of approximately 2,000–4,000 meters run from north to south lay in the middle of the Taiwan Island. Among the rivers originated from the Central Mountain Range, the Kaoping

\* Corresponding author.

Tel.: +886-7-5252000 ext. 4409; Fax: +886-7-5254409  
E-mail address: ycsngi@mail.nsysu.edu.tw

River is the only one flowing southward in the island. Moreover, wind direction also plays a crucial role in the occurrence of ADEs caused by the outflow of typhoon circulation, because the wind can circulate with anticyclones and blow air streams northward.

Additionally, the watershed of the Kaoping River is the largest in Taiwan Island, covering an area of approximately 3,257 km<sup>2</sup>. The water level of the Kaoping River drops rapidly following the rainy days in summer. More than half of the riverbed can turn into exposed bare lands due to high solar radiation from the sunlight, potentially resulting in ADEs in southern Taiwan. This is in stark contrast to other rivers in Taiwan Island, where their ADEs occur mostly in the seasons from late winter to early spring (Lin et al., 2007; Kuo et al., 2010). At present, the Central Weather Bureau (CWB) of Taiwan is capable of forecasting the date of northeasterly Monsoons arriving at Taiwan Island. However, the CWB has difficulties in predicting the occurrences of ADEs originating from the riverbeds, though it can precisely forecast the typhoon pathways. Accordingly, up to date, the occurrence of ADEs along the Kaoping River is still unpredictable. In the past, the residents living by the Kaoping River have experienced ADEs without warning in most cases. Previous study reported that exposure to high levels of PM<sub>10</sub> could cause potential health risks of respiratory and cardiovascular hospitalization during the ADEs (Meng et al., 2007).

In addition to natural aeolian dust emitted from the drought bare lands of riverbeds, several anthropogenic sources adjacent to the Kaoping River could also emit PM<sub>10</sub> to the ambient air. There are three major industrial complexes (e.g., the Linyuan industrial complex, Dafa industrial complex, and Pingtung export processing zone)

located at the downstream of the Kaoping River (Tsai et al., 2006; Tsai et al., 2008, 2011), which emit a huge amount of PM<sub>10</sub> regularly to the atmosphere with or without the occurrence of ADEs. Accordingly, the present study aims to identify the chemical characteristics of aeolian dust sampled during the ADE in southern Taiwan, to locate the hot spots highly affected by ADEs, and to determine the contribution of ADEs to ambient particulate air quality along the Kaoping River.

## METHODOLOGIES

### *Sampling Protocol of PM<sub>10</sub>*

In the present study, ambient PM<sub>10</sub> was manually collected with high-volume samplers (TISCH 6070DV) at four sampling sites (KA, KB, PC, and PD) (see Fig. 1(a)) in a sampling network on regular days and in intensive periods during and after the ADE. Regular sampling of ambient PM<sub>10</sub> was conducted to sample 24-hr PM<sub>10</sub> starting from 8:00 a.m. (local time) on July 7–14, 2012, while intensive sampling of ambient PM<sub>10</sub> was conducted in two stages, during and after ADE, at four sampling sites during the Typhoon Doksur on June 29–30, 2012.

The forward trajectory of Typhoon Doksur passing through the western Pacific Ocean is illustrated in Fig. 1(b). The sampling flow rate of high-volume samplers was operated at 1.4 m<sup>3</sup> min<sup>-1</sup> based on the standard method of NIEA A102.12A. Stage I was conducted from 13:00 p.m. to 16:00 p.m. on June 29, 2012, while Stage II was carried out from 16:00 p.m. to 8:00 a.m. of the sequential day after the ADE on June 29–30, 2012. In addition, chemical fingerprints of alluvial soils sampled at the bare lands on the riverbed along the Kaoping River. Quartz fiber filter was used to

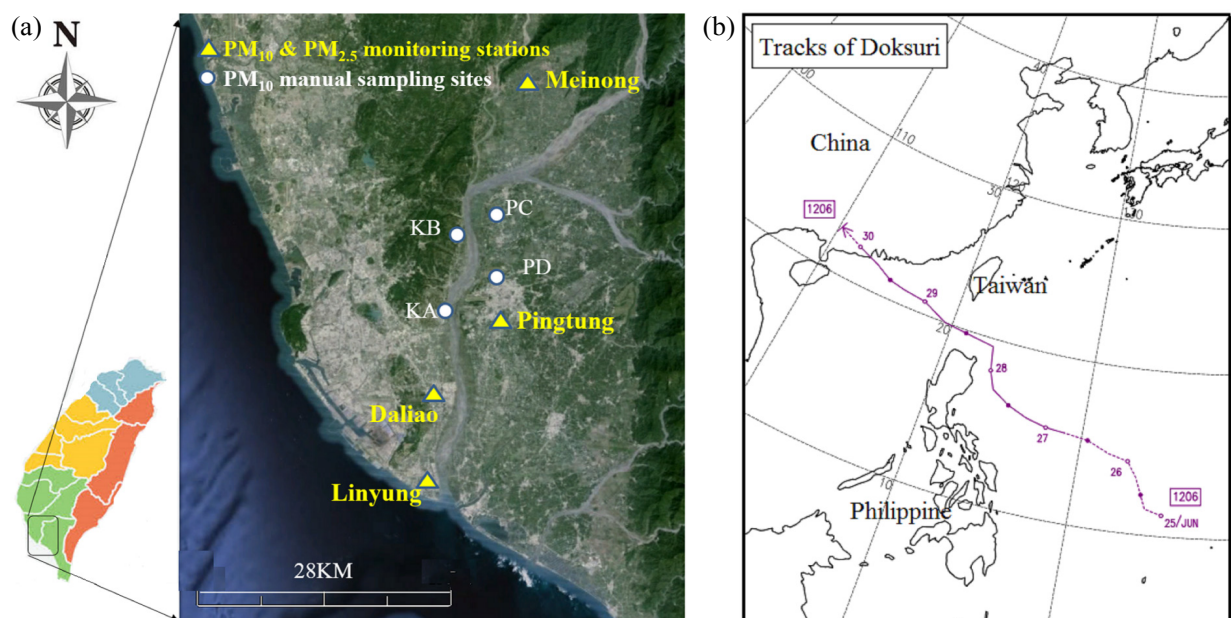


**Fig. 1.** (a) Location of PM<sub>10</sub> manual sampling sites (KA: Kaoping River Weir Management Center; KB: Fo-Guang-Shan Buddha Memorial Museum; PC: Yutian Elementary School; PD: Yu-Suei Branch Campus of Huei-Nung Elementary School) and Ambient Air Quality Monitoring Stations along the Kaoping River Valley in Southern Taiwan. (b) The tracks of Typhoon Doksur occurred on June 25–30, 2012.

collect PM<sub>10</sub> samples for further chemical analysis. The quality assurance and quality control (QA/QC) for sampling and chemical analysis of PM<sub>10</sub> are shown as Methods in Supplementary Information.

### **Chemical Analysis of PM<sub>10</sub>**

After sampling, conditioning, and weighing of PM<sub>10</sub>, chemical composition including water-soluble ionic species, metallic elements, and carbonaceous contents were analyzed for PM<sub>10</sub> samples collected on regular days and in the intensive periods during and after the ADE. All quartz fiber filters were initially divided into four identical portions. One-quarter of the quartz fiber filter was put inside a 15-mL bottle made of polyethylene (PE) to extract and analyze the water-soluble ions. Each bottle was filled with distilled de-ionized water (D.I. H<sub>2</sub>O) and then vibrated ultrasonically for 60 min. The mixed solution obtained from each bottle was then filtered to avoid the separation column damped for extending the life span of the analytical instrument. The concentrations of major anions (i.e., fluoride (F<sup>-</sup>), chloride (Cl<sup>-</sup>), sulfate (SO<sub>4</sub><sup>2-</sup>) and nitrate (NO<sub>3</sub><sup>-</sup>)) and major cations (i.e., ammonium (NH<sub>4</sub><sup>+</sup>), potassium (K<sup>+</sup>), sodium (Na<sup>+</sup>), calcium (Ca<sup>2+</sup>) and magnesium (Mg<sup>2+</sup>)) were measured with an ion chromatography (IC) (Dionex, DX-120). Another quarter of the quartz fiber filter was used to analyze metallic elements by initially digesting them in a 20 mL mixed acid solution (HNO<sub>3</sub>:HCl = 3:7) at 150–200°C for 2 hr, and then diluting the solution to 50 mL with distilled de-ionized water (D.I. H<sub>2</sub>O). The metallic elements of PM<sub>10</sub> including sodium (Na), calcium (Ca), aluminium (Al), iron (Fe), magnesium (Mg), potassium (K), zinc (Zn), chromium (Cr), titanium (Ti), manganese (Mn), cadmium (Cd), nickel (Ni), and lead (Pb) were analyzed with an inductively coupled plasma-atomic emission spectrometer (ICP-AES) (Perkin Elmer, 2400 Series II).

Two-eighths of the quartz fiber filters were further used to analyze the carbonaceous content of PM<sub>10</sub>. Carbonaceous contents including elemental, organic, and total carbons (OC, EC, and TC) were measured with an elemental analyzer (EA) (Carlo Erba, Model 1108). Prior to sampling, the quartz fiber filters were initially pre-heated in 900°C for at least 1.5 hr to remove potential carbon impurities from the filters. After PM<sub>10</sub> sampling, one-eighth of the quartz fiber filter was heated using nitrogen gas at 340–345°C for at least 43 min to expel organic carbon (OC) fraction, and the concentration of elemental carbon (EC) was determined. Previous studies reported that PM<sub>10</sub> samples exposed at a temperature of 340°C for 43 mins could effectively minimize the pre-combustion charring OC (Lavanchy et al., 1999). Another eighth of the quartz fiber filter was analyzed without preheating to determine the concentration of total carbon (TC). The concentration of organic carbon (OC) was then determined by subtracting EC from TC (Tsai et al., 2010; Li et al., 2013).

### **Chemical Mass Balanced (CMB) Receptor Model**

Previous studies reported that source identification and apportioning of PM had been recognized as one of the curial measures to quantify the major contributors of PM

to improve the poor particulate air quality (Cao et al., 2009; Nayebare et al., 2016; Taiwo et al., 2016). Studies have used several measures to assess the comparative performance of various source apportionment techniques namely, CMB receptor modelling, positive matrix factorization, principal component analysis (PCA), absolute principal component analysis, and targeted factor analysis (Hopke et al., 2006; Brook et al., 2007; Nayebare et al., 2016). In the present study, we solely use CMB receptor model to resolve source identification and apportionment of potential emission sources because of the limited PM<sub>10</sub> samples (Tsai et al., 2010; Li et al., 2015). Typically, the CMB receptor model has been widely applied to distinguish the contributions from four to eight types of sources (Engelbrecht et al., 2013). The principle of CMB receptor model and the details of source profiles are presented as Methods in Supplementary Information.

### **Space Analysis Software (SURFER)**

SURFER version 8.0 software has been commonly used to plot 3D spatial diagrams. An XYZ data file is created in the SURFER worksheet, a grid file is produced using Point Kriging Gridding (PKG) method, and a series of maps were formed in SURFER plot document. The relationship of XYZ data files, grid files, and maps are then transformed to 3D spatial diagrams. The present study aims to identify the hot spots where were obviously affected by the ADEs (Tsai et al., 2010; Li et al., 2015). Thus, we chose only 2D spatial plotting scheme to plot the hourly PM<sub>10</sub> concentration contours from 9:00 a.m. to 4:00 p.m. on June 29, 2012, covering the overall view on the spatiotemporal distribution of PM<sub>10</sub> along the Kaoping River Valley.

### **Weather Research and Forecasting (WRF) Model**

Weather Research and Forecasting Model (WRF version 3.7) is a proposed meteorological model developed by NOAA/ESRL (Sun et al., 2016), which was used to simulate the wind fields during and after the ADE in the studied area in this study. WRF model provides a friendly used environment for massively parallel computation by the improved characteristics of non-hydrostatic air flow fields and offers various choices for physical parameterizations (Huang et al., 2013; Shahid et al., 2015). The details of WRF model are not described herein in this paper since the principles of the model are elsewhere.

### **Statistical Analysis Methods**

Data statistical analysis was performed using the IBM SPSS 19.0 (Statistical Product and Service Solutions) software package. For limit alluvial soil samples collected from the bare lands on the riverbeds along the Kaoping River, nonparametric statistics are more applicable than the parametric statistics. Thus, the Kruskal-Wallis test assesses significant differences in a continuous dependent variable by group independent variables (variables with three or more groups). It is assumed that the distribution of each group is not normal and the variance in the scores differs significantly for each group. Accordingly, the present study employed the Kruskal-Wallis test to compare the metallic

elements in the alluvial soils collected from the Kaoping River (Taiwan EPA, 2008; Kuo et al., 2010).

## RESULTS AND DISCUSSION

### *Spatiotemporal Variation of PM<sub>10</sub> Concentration on Regular Days and during and after the ADE*

Appreciable ADE occurring on June 29, 2012, was recorded by the CWB, when Typhoon Doksur passed through the Bashi Channel with an anticyclone outflow circulation, as shown in Fig. 1(b). A separate outflow caused by Typhoon Doksur entered the Kaoping River Valley through its estuary from the south because the Kaoping River flows southward. Consequently, strong winds blew dry alluvial soils from the bare lands over the riverbeds along the Kaoping River during the ADE. According to four TEPA's Air Quality Monitoring Stations (AQMSs) aside from the Kaoping River, as shown in Fig. 1(a), the wind speeds, wind directions, and PM<sub>2.5</sub> and PM<sub>10</sub> concentrations measured on June 29, 2012, are illustrated in Fig. 2. It shows a variation of hourly PM<sub>2.5</sub> and PM<sub>10</sub> concentrations recorded on June 29, 2012. We speculated the spatiotemporal distributions of PM<sub>2.5</sub> and PM<sub>10</sub> over the Kaoping River Valley during the ADE. The highest hourly PM<sub>10</sub> concentration of 1,488 µg m<sup>-3</sup> was recorded at 10:00 a.m. at the Daliao AQMS on June 29, 2012. The 24-h PM<sub>10</sub> showed significant temporal variability with average ( $414.5 \mu\text{g m}^{-3} \pm 432.4 \mu\text{g m}^{-3}$ ) exceeding the 24-h PM<sub>10</sub> Air Quality Standard ( $125 \mu\text{g m}^{-3}$ ) by 3.3 fold at the Daliao AQMS on June 29, 2012. Compared to the monthly PM<sub>10</sub> ( $39.8 \mu\text{g m}^{-3} \pm 6.8 \mu\text{g m}^{-3}$ ), shown in Fig. S1 in Supplementary File, at the Daliao AQMS on regular days, the average PM<sub>10</sub> concentration was over 10-fold on June 29, 2012. While the Typhoon Doksur gradually moved away from Bashi Channel on June 29–30, 2012, the PM<sub>10</sub>

concentration at Daliao AQMS drastically decreased to  $33.5 \mu\text{g m}^{-3} \pm 9.9 \mu\text{g m}^{-3}$  after the ADE correspondingly. In addition, Table 1 presents the concentration of PM<sub>10</sub> measured at four manual sampling sites (i.e., KA, KB, PC, and PD). In particular, Site KA had the highest hourly average PM<sub>10</sub> concentration of  $677.4 \mu\text{g m}^{-3}$  during the ADE, indicating that PM<sub>10</sub> concentration rose as high as 30-fold higher than the average PM<sub>10</sub> concentration on regular days ( $22.7\text{--}37.9 \mu\text{g m}^{-3}$ ). Site KB was highly affected by the ADE with an hourly PM<sub>10</sub> concentration of  $216.1 \mu\text{g m}^{-3}$ , which was consistent with the PM<sub>10</sub> concentration obtained from the EPA Ambient Air Quality Stations. Similar PM<sub>10</sub> levels were observed on the left bank of the Kaoping River. Low hourly average PM<sub>10</sub> concentrations at Sites PC and PD located on the left bank of the Kaoping River were as low as  $73.4 \mu\text{g m}^{-3}$  and  $97.6 \mu\text{g m}^{-3}$ , respectively.

This study further compared the manual sampling data and the monitoring data to plot the concentration contours of PM<sub>10</sub> by using SURFER spatial software and WRF model as shown in Figs. 3(a)–3(x) and 4, respectively. To figure out the causes of the ADE occurred on June 29, 2012, this study simulated the near ground surface wind fields along the Kaoping River in southern Taiwan, an analysis of the weather (synoptic) charts above 10 meters from the ground surface. Supposedly, as the mesoscale of weather chart, relating to a meteorological phenomenon approximately 10 to 1,000 kilometers in the horizontal extent, can effectively depict the dynamic variations of the atmospheric state (e.g., the distribution and characteristics of air masses, the different baric systems such as cyclones, anticyclones, troughs, crests, and so on), an intergraded analysis facilitated further understanding the development of the transporting aeolian dust under certain weather condition in the studied regions during the typhoon season. Figs. 3(a)–3(x) demonstrate the simulated surface wind

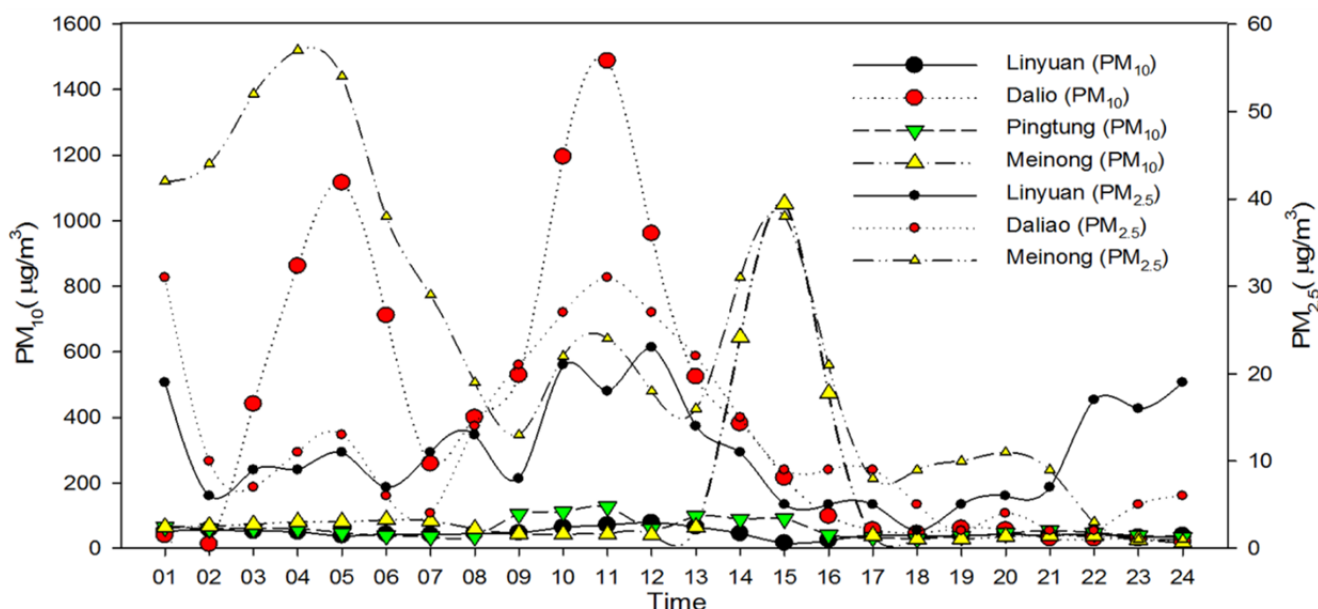


**Fig. 2.** PM<sub>2.5</sub> and PM<sub>10</sub> concentrations on June 29, 2012 recorded by four Taiwan Environmental Protection Administration's Air Quality Monitoring Stations along the Kaoping River.

**Table 1.** Variation of PM<sub>10</sub> concentration measured at different sampling sites along the Kaoping River on regular days and during the ADE.

Sampling Sites	Latitude/Longitude/Altitude (m)	Brief Descriptions	Sampling Periods	PM <sub>10</sub> ( $\mu\text{g m}^{-3}$ )
Right Bank	KA 22°40'34"/120°25'37"/13	Suburban area directly exposes to Kaoping River	Regular days	27.2 ± 3.79
			Stage I	677.4
			Stage II	90.2
			Regular days	25.9 ± 4.97
Right Bank	KB 22°44'45"/120°26'25"/12	Busy traffics from visitors	Stage I	216.1
			Stage II	69.9
			Regular days	22.1 ± 4.97
			Stage I	73.4
Right Bank	PC 22°46'47"/120°29'38"/16	Intensive resident district and nearby gravel processing plants	Stage II	39.3
			Regular days	37.9 ± 5.96
	PD 22°42'57"/120°28'57"/10	Residential and traffic mixture area	Stage I	97.6
			Stage II	53.2

a. Regular days: 24-hr PM<sub>10</sub> from 8:00 a.m. on July 7–14, 2012.

b. Stage I: 3-hr PM<sub>10</sub> from 1:00 p.m. to 4:00 p.m. on June 29, 2012.

c. Stage II: 16-hr PM<sub>10</sub> from 4:00 p.m. to 8:00 a.m. on June 29–30, 2012.

fields in the ADE occurred along the Kaoping River in southern Taiwan on June 29, 2012, from 1:00 a.m. to 11:00 p.m. Air masses were in the turbulent conditions between Kaohsiung City and Pingtung County during the period of 1:00 a.m. to 6:00 a.m. The influences of outflow circulations caused by Typhoon Dokuri, a low-pressure central system, were obviously investigated at the open seas of southern Taiwan in the daytime from 7:00 a.m. to 6:00 p.m. As the Typhoon Dokuri moved gradually away from Taiwan Island, the motion of air masses was from the east-side open seas to the west-side open seas of southern Taiwan correspondingly. The prevailing winds have also progressively turned from westward to northwestward along the Kaoping River Valley during the period of 7:00 a.m. to 12:00 p.m., then during the following period, southern winds dominated until the end of the day. Since the wind fields were simulated at the height of 10 meters height from the surface of the Kaoping River, the simulated prevailing southwestern winds from 7:00 a.m. to 12:00 p.m. on the surface, where alluvium soils exist, should be dominated by southern winds. Additionally, the hills located along the right bank were another factor to restrict the surface wind directions along the Kaoping River.

While the speed of southern wind increased along the Kaoping River Valley, the air mass could blow the aeolian dust fugitively from the bare lands in the estuary of the Kaoping River, which dramatically influence the ambient particulate air quality. It reasonably explained why high PM<sub>10</sub> concentrations occurred at the Dalio and Meinong AQMSs were sequentially affected by blowing aeolian dust, particularly under the calm wind conditions as shown in Fig. 4. A superimposition phenomenon was supposedly observed at the Meinong AQMS after the ADE affected by the combined effects of cross-boundary transportation, from Bashi Channel to the inlands of Kaoping River, and local emission sources at the downstream areas on both sides of river banks in the Kaoping River. In brief, the cause of ADE was mainly conducive to the dominant southern

winds during the typhoon season rather than those during the northeastern monsoons in winter and early spring as well. The observation of emerging ADE is worthy of being emphasized at the Kaoping River due to its particular flow direction, from north to south. Conversely, the wind directions and wind speeds observed at the Linyuan AQMS could be further adapted to early warning for the ADEs in the upstream of the Kaoping River.

#### **Chemical Constituents of PM<sub>10</sub> on Regular Days and during and after the ADE**

Fig. 5(a) illustrates the mass concentrations of water-soluble ions (WSIs) in PM<sub>10</sub> sampled on regular days, as well as during and after the ADE. The WSI fractions of PM<sub>10</sub> accounted for 38.7–42.1%, 34.0–36.5%, and 37.0–44.2%, respectively, on regular days, and the periods during and after the ADE. It showed that the mass ratios of WSIs and PM<sub>10</sub> (WSI/PM<sub>10</sub>) during the ADE were commonly lower than those on regular days and the period after the ADE, however, there were no differences of WSI/PM<sub>10</sub> between the regular days and after the ADE. It was mainly attributed to the fact that huge amount of aeolian dust were fugitively suspended to the ambient air during the ADE. No matter which periods, the most abundant WSIs of PM<sub>10</sub> were SO<sub>4</sub><sup>2-</sup>, NO<sub>3</sub><sup>-</sup>, and NH<sub>4</sub><sup>+</sup>, indicating that secondary inorganic aerosols (SIAs) were the major portion of PM<sub>10</sub>, in concurrence with previous studies (Cao *et al.*, 2009; Tsai *et al.*, 2011; Zhao *et al.*, 2016). Moreover, SIAs (i.e., the sum of NO<sub>3</sub><sup>-</sup>, SO<sub>4</sub><sup>2-</sup>, and NH<sub>4</sub><sup>+</sup>) constituted 69.7–73.1%, 66.2–68.6%, and 64.8–72.5% of the total WSIs on regular days, and the periods during and after the ADE, respectively. Previous studies have indicated that SIAs formed in the atmosphere mostly through chemical reactions of precursors (i.e., NO<sub>x(g)</sub>, SO<sub>2(g)</sub>, and NH<sub>3(g)</sub>) and mainly formed ammonium nitrate (NH<sub>4</sub>NO<sub>3</sub>) and ammonium sulfate ((NH<sub>4</sub>)<sub>2</sub>SO<sub>4</sub>) (Han *et al.*, 2007; Tsai *et al.*, 2011; Sun *et al.*, 2016; Zhao *et al.*, 2016). The formation of SIAs strongly depends on atmospheric conditions and the

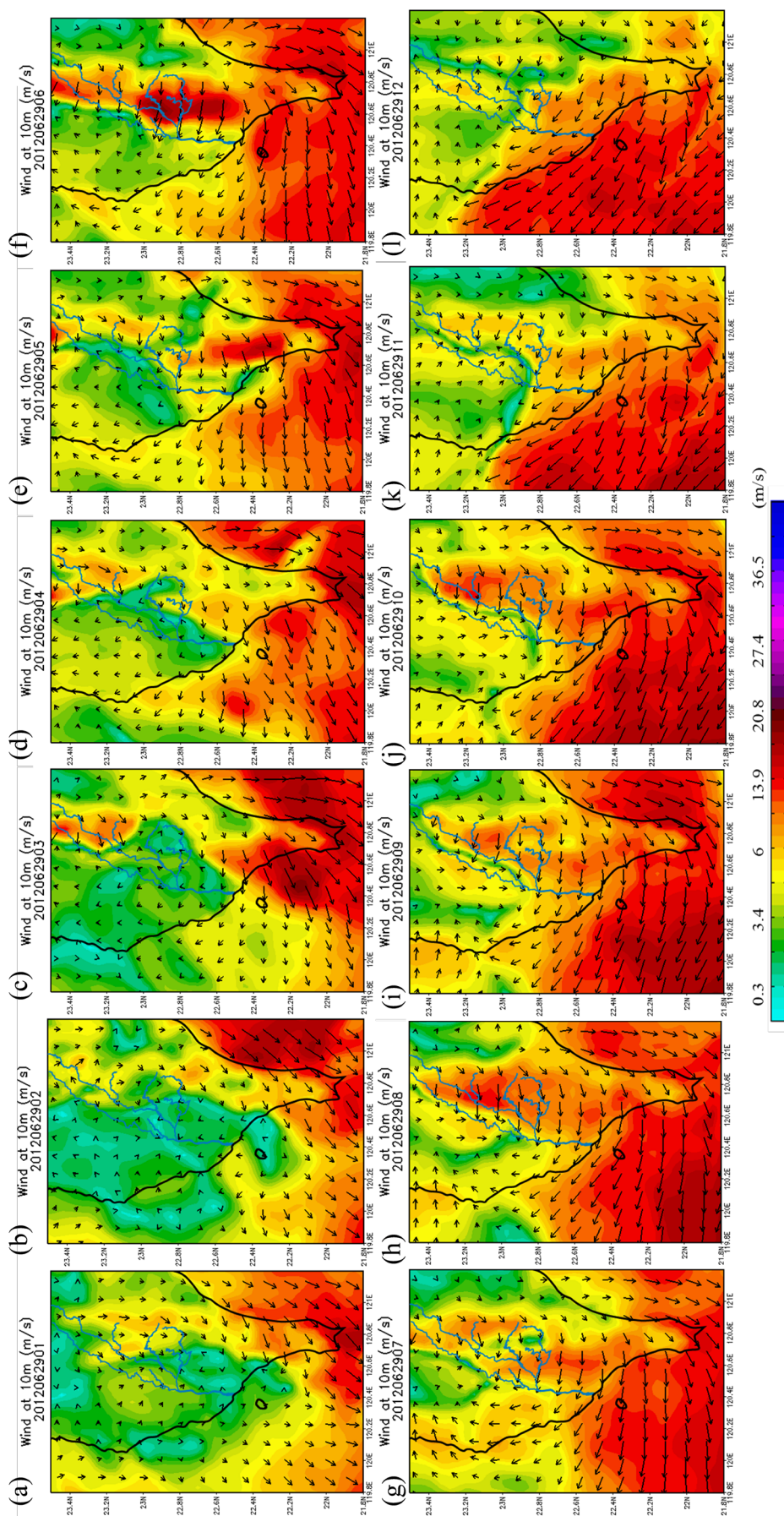


**Fig. 3.** (a)–(l) Simulated hourly surface wind fields in the aeolian dust episode occurred along the Kaoping River in southern Taiwan from 01:00 a.m. to 12:00 p.m. on June 29, 2012.

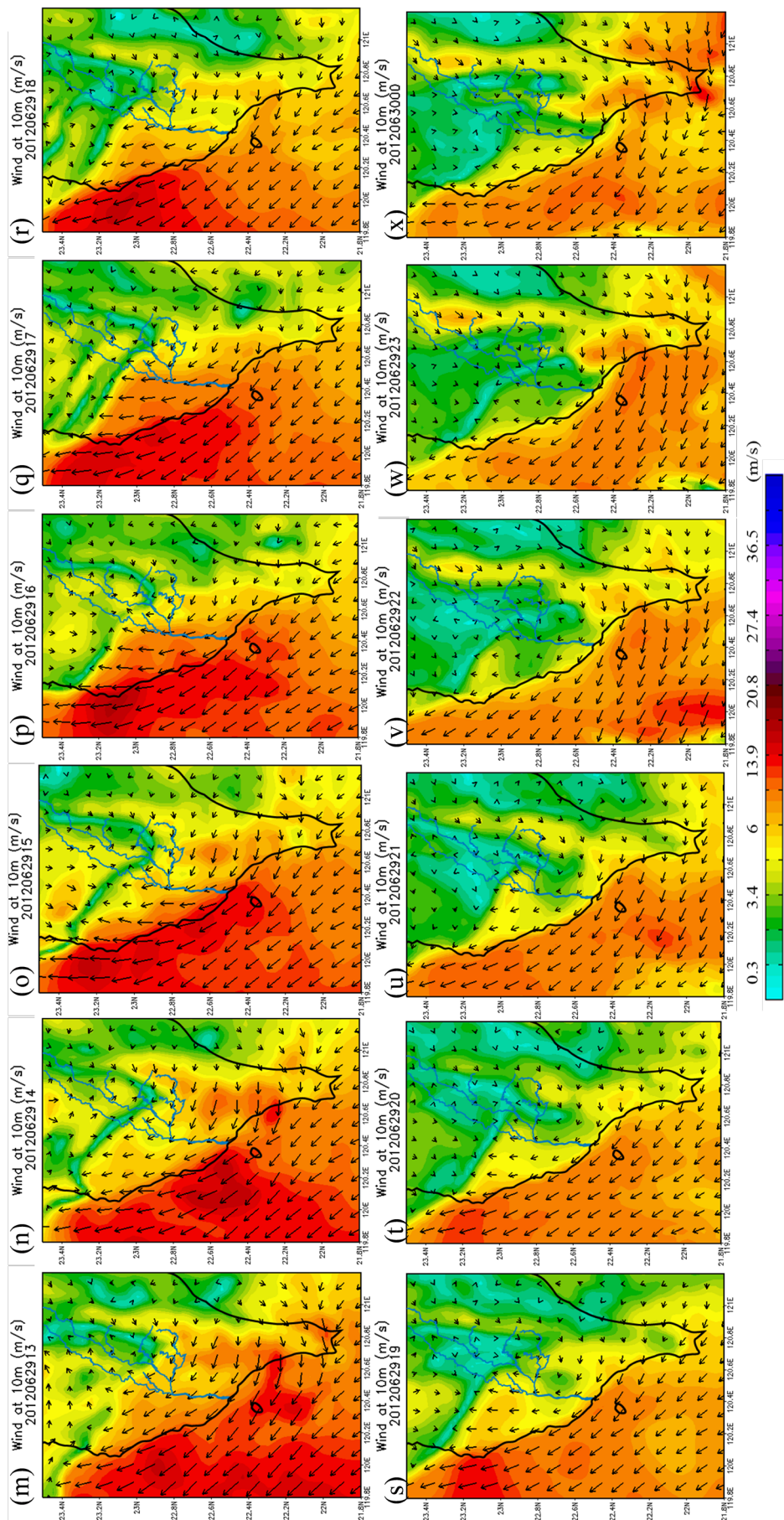


**Fig. 3.** (m)–(x) Simulated hourly surface wind fields in the aeolian dust episode occurred along the Kaoping River in southern Taiwan from 13:00 p.m. to 24:00 p.m. on June 29, 2012.

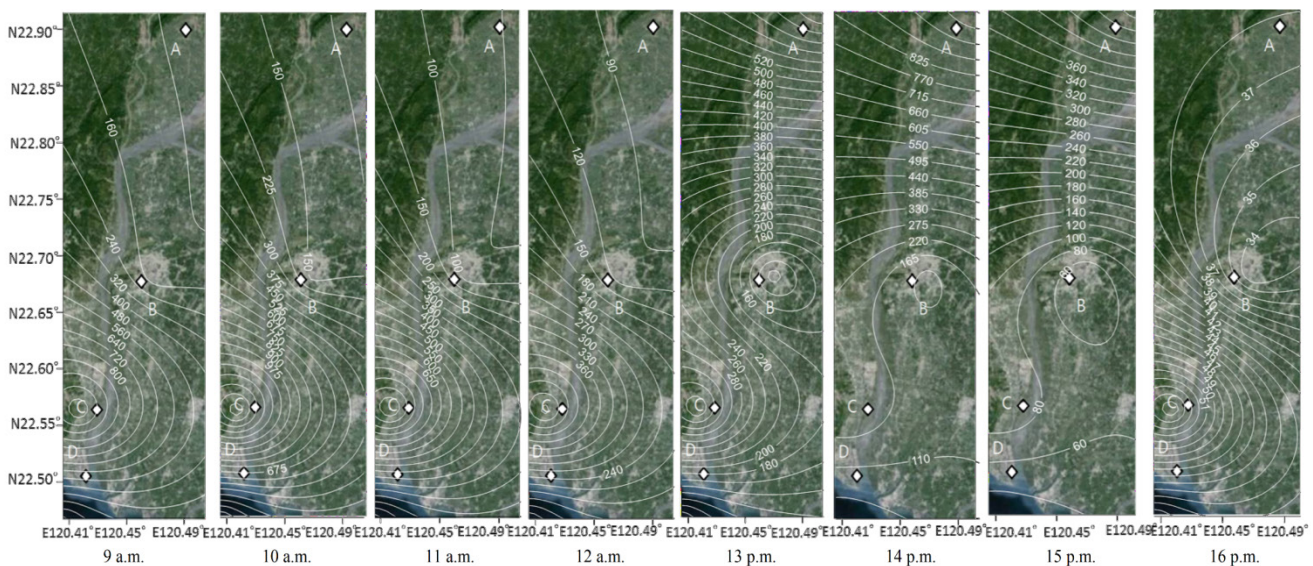


**Fig. 4.** Hourly spatiotemporal variation of  $\text{PM}_{10}$  concentration along the Kaoping River Valley during the ADE on June 29, 2012.

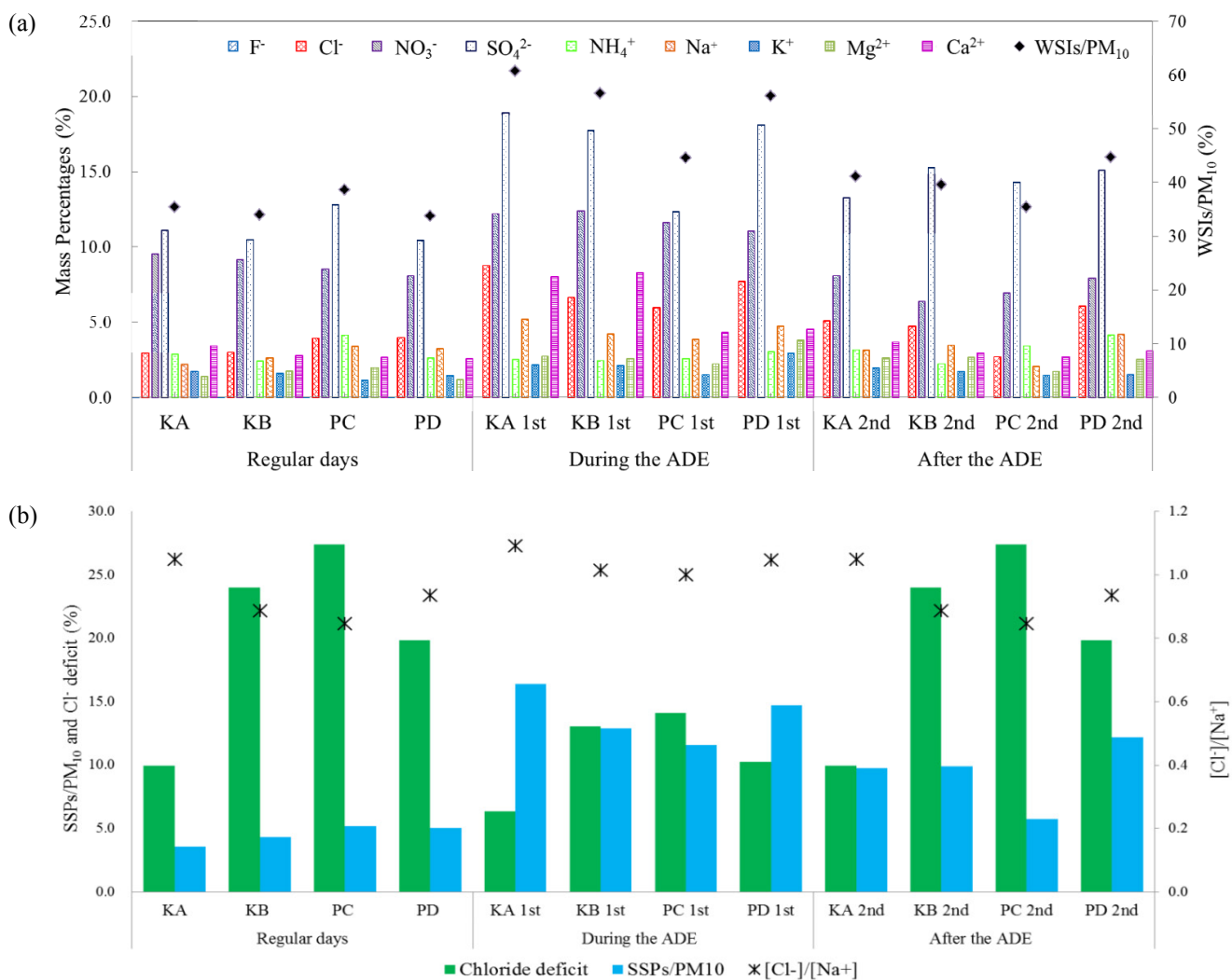


**Fig. 5.** (a) Mass percentage of water-soluble ionic species of  $\text{PM}_{10}$  and (b) the chloride deficit and the molar ratio of  $[\text{Cl}^-]/[\text{Na}^+]$  in  $\text{PM}_{10}$  along the Kaoping River on regular days and in the periods of the ADE.

availability of precursor gasses. Ammonia first neutralizes sulfuric acid to form ammonium bisulfate ( $(\text{NH}_4)\text{HSO}_4$ ) and ammonium sulfate ( $(\text{NH}_4)_2\text{SO}_4$ ). In the present study, the mass fraction of WSIs in  $\text{PM}_{10}$  exhibited a descending tendency (defined as a spatiotemporal variation) when a considerable amount of dried aeolian dust existed in the atmosphere during the ADE. The mass ratios of WSIs to  $\text{PM}_{10}$  during the ADE were lower than those on regular days and after the ADE in the same region (Tsai et al., 2006; Tsai et al., 2008, 2010), indicating that this might be related to meteorological conditions (Wang et al., 2015).

Fig. 5(b) shows that the molar ratios of  $[\text{Cl}^-]/[\text{Na}^+]$  were in the range of 0.74–0.88 on regular days, 0.95–1.02 during the ADE, and 0.77–0.85 after the ADE, respectively. The molar ratios of  $[\text{Cl}^-]/[\text{Na}^+]$  during the ADE were generally higher than those on regular days and after the ADE, however, there were no differences of  $[\text{Cl}^-]/[\text{Na}^+]$  between the regular days and the period after the ADE. The results indicated that oceanic spray was a dominant factor with increasing wind speeds due to strong winds blown by the outflow circulation of Typhoon Doksuri during the period of ADE (Kumar et al., 2008; 2012). This study estimated the amounts of sea-salt particles (SSPs) by using Eq. (1), which is appropriate for investigating the proportions of SSPs in  $\text{PM}_{10}$  (Quinn et al., 2000):

$$\text{SSPs} = 1.47 \times [\text{Na}^+] + [\text{Cl}^-] \quad (1)$$

where 1.47 is the mass ratio of  $([\text{Na}^+] + [\text{K}^+] + [\text{Mg}^{2+}] + [\text{Ca}^{2+}] + [\text{SO}_4^{2-}] + [\text{HCO}_3^-])/[\text{Na}^+]$ . According to the SSPs estimated by Eq. (1), we revealed that the mass percentages of SSPs to  $\text{PM}_{10}$  ( $\text{SSPs}/\text{PM}_{10}$ ) accounted for 11.66–16.47% during the ADE, which were obviously higher than those on regular days (3.93–5.17%) and in the period after the ADE (5.74–12.29%). The results shown in Fig. 5(b) indicated that Eq. (1) can reasonably explain the relatively higher SSPs in  $\text{PM}_{10}$  during the ADE. For the events of ADEs accompanied by typhoon outflow, strong winds could blow huge amounts of SSPs from the Bashi Channel to the

Kaoping River Valley (Park et al., 2004; Tsai et al., 2010).

Crustal materials (CMs), anthropogenic sources, and oceanic sprays are major sources of  $\text{PM}_{10}$  in the coastal industrial regions (Chester et al., 2000; Yuan et al., 2006; Wang et al., 2015). Previous studies have reported that crustal-origin elements (e.g., Al, Ca, and Fe) are abundant in the background particulate matter (Ni et al., 2013; Li et al., 2015; Nayebare et al., 2016). The metallic elements of  $\text{PM}_{10}$  collected on regular days and the periods during and after the ADE are illustrated in Fig. 6. It shows that the most abundant metallic elements of  $\text{PM}_{10}$  were crustal elements (i.e., Al, Fe, Mg, and Ca). The crustal materials of  $\text{PM}_{10}$ , as high as 87.6% during the ADE, were commonly higher than those on regular days (77.7%) and after the ADE (80.1%). The contribution of crustal materials to  $\text{PM}_{10}$  increased dramatically during the ADE because they are the main metallic component of natural soils (Taiwan EPA, 2009; Chen et al., 2015; Wang et al., 2015). Furthermore, aeolian dust emitted from the Kaoping River Valley in southern Taiwan were mainly observed in summer and fall, which are different from Asian dust commonly occurred in winter and spring (Tsai et al., 2006). Asian dust is mainly originated from Chinese Loess Plateau and deserts (Tsai et al., 2006), whereas aeolian dust is emitted from the bare lands along the Kaoping River in southern Taiwan. Consequently, aeolian dust occurred in southern Taiwan during the ADE (Stage I) should have their unique chemical characteristics (Chow et al., 2002; Taiwan EPA, 2009; Taiwan WRA, 2009). For instance, Sun et al. (2016) reported that Pb might be fugitively emitted from paved and unpaved roads where roadside leaded soils were originally deposited from the exhausts of motor vehicles using leaded gasoline. Moreover, the gravel plants are intensively distributed at the upstream of the Kaoping River. Thus, we speculated that Pb emitted from vehicular exhausts might be the major source of Pb in  $\text{PM}_{10}$  (Xu et al., 2014), because diesel fuel was used for trucks to convey gravel for building or road construction. However, the particulate Pb could be also emitted from coal-fired boilers, municipal and industrial

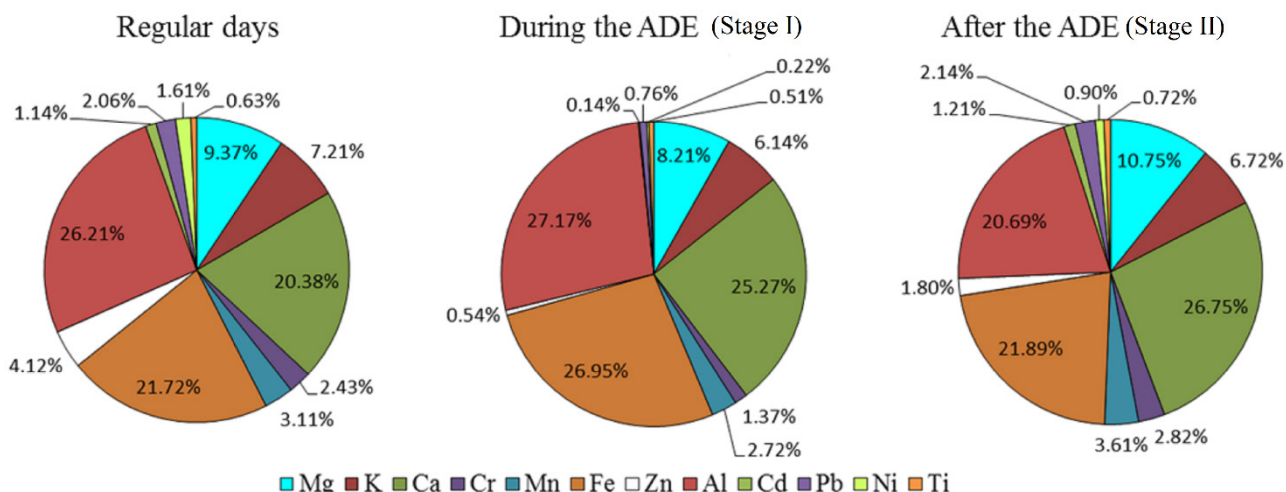


**Fig. 6.** Mass percentages of eleven metallic elements along the Kaoping River on regular days and the periods during and after the ADE.

waste incinerators (Sun *et al.*, 2006), metal brake wear (Sternbeck *et al.*, 2002), and industrial activities such as metallurgical processes (Kabala and Singh, 2001; Shtiza *et al.*, 2005).

Previous studies have reported that the mass ratios of organic carbon to elemental carbon (OC/EC) can be used to identify the potential formation of secondary organic aerosols (SOAs) when the OC/EC ratios exceed 2.1–2.2 (Meng *et al.*, 2007; Tsai *et al.*, 2011; Li *et al.*, 2013a, b). Fig. 7 illustrates a comparison of OC/EC on regular days and during the ADE. It showed that the OC/EC ratios ranging from 1.18 to 1.35 during the ADE were obviously lower than those on regular days and in the period after the ADE due to the influences of Typhoon Doksumi. Thus, OC was the dominant carbonaceous content of resuspended alluvial soils, which was slightly higher than EC. The results implied that the bare areas on the riverbed might have been the major contributors to PM<sub>10</sub> during the ADE. Moreover, the weather conditions (i.e., prevailing southern winds with a dilution effect) during the ADE were unfavorable for the formation of secondary organic aerosols (SOAs), resulting in the values being apparently lower than those on regular days and in the period after the ADE. The mass ratios of OC/EC for the Kaoping River on regular days and in the period after the ADE were 1.87–2.46 and 1.51–2.48, respectively. PM<sub>10</sub> emitted from the bare lands on the riverbed should be a dominant source of ADE. Site PD had the highest mass ratio of OC/EC (2.48), which was affected by anthropogenic sources such as heavy oil boilers and leather industries in Pingtung County.

#### Fingerprint of PM<sub>10</sub> Resuspended from Alluvium Soils

This study took alluvium soil samples from the fluvial basin at five sites along the Kaoping River. A total of 30 representative soil samples were regularly collected from the bare lands where great amounts of aeolian dust were fugitively emitted to the air. The chemical fingerprints of PM<sub>10</sub> that were resuspended from the alluvium soils are

illustrated in Fig. 8. The carbonaceous content of resuspended PM<sub>10</sub> was one of the richest chemical content, with the mass percentages of 10.7 ± 2.81% and 9.60 ± 2.51% for OC and EC, respectively. Among the carbonaceous contents, the amount of OC was higher than that of EC in the resuspended PM<sub>10</sub>. OC- and EC-containing particulates are commonly emitted from incomplete combustion of carbonaceous fuels as well as the photochemical reactions. EC is released only from combustion processes and thus is always a primary material (Cao *et al.*, 2003; Han *et al.*, 2007; Tsai *et al.*, 2012), while OC can be directly emitted to the atmosphere in particulate form, or formed in the atmosphere by gas-to-particle conversion during the photochemical reaction processes (Seinfeld and Pandis, 1998; Tsai *et al.*, 2011). The influences of various anthropogenic sources situated near the alluvium soil sampling sites along the Kaoping River resulted in a high variance of OC and EC in alluvium soils. It was attributed to the following two reasons: (1) OC and EC were mainly emitted from anthropogenic sources at nearby industrial complexes, of which the production processes required a considerable amount of fossil fuels (e.g., the Linyuan and Dafa industrial complexes and the Pingtung export processing zone) in the downstream region of the Kaoping River. (2) A substantial amount of gravel has been persistently eroded by flooding from the upstream to the downstream areas during the Typhoon Morakot in 2009, resulting in large areas of bare lands distributed on the downstream riverbed along the Kaoping River. Therefore, routine dredging is required to conserve the capacity of the water course of the Kaoping River in the rainy season. Hundreds of trucks conveyed gravels back and forth among the water course and the excavation sites nearby the riverbank during the drought season. Consequently, a certain amount of elemental carbon emitted from the exhausts of the gravel conveying trucks tends to deposit on the surface of alluvium soils at the bare lands along the Kaoping River (Cao *et al.*, 2001; Han *et al.*, 2007).

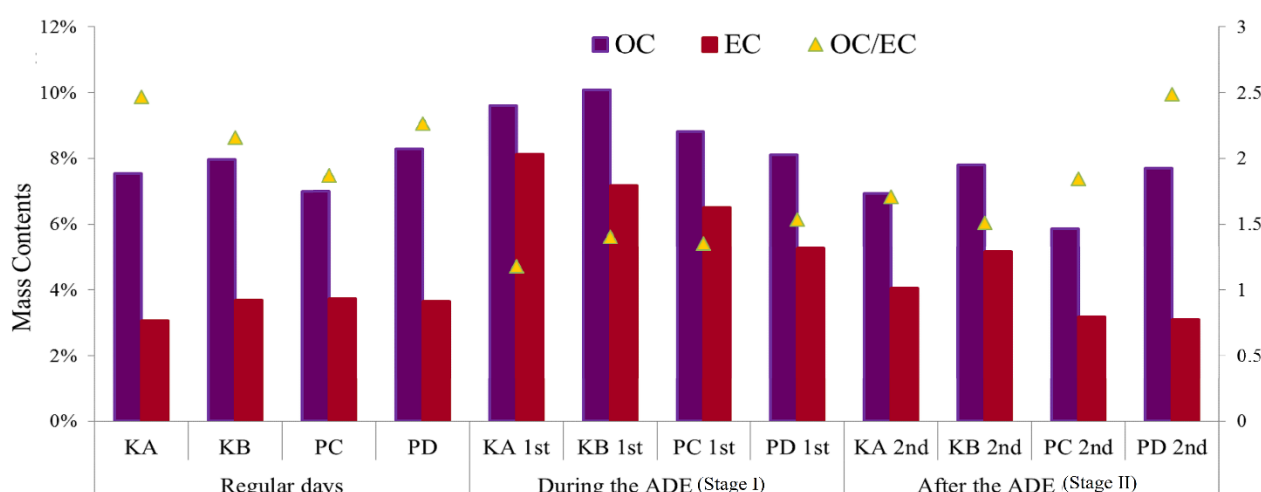


**Fig. 7.** Carbonaceous contents of OC and EC sampled along the Kaoping River on regular days and the periods during and after the ADE.

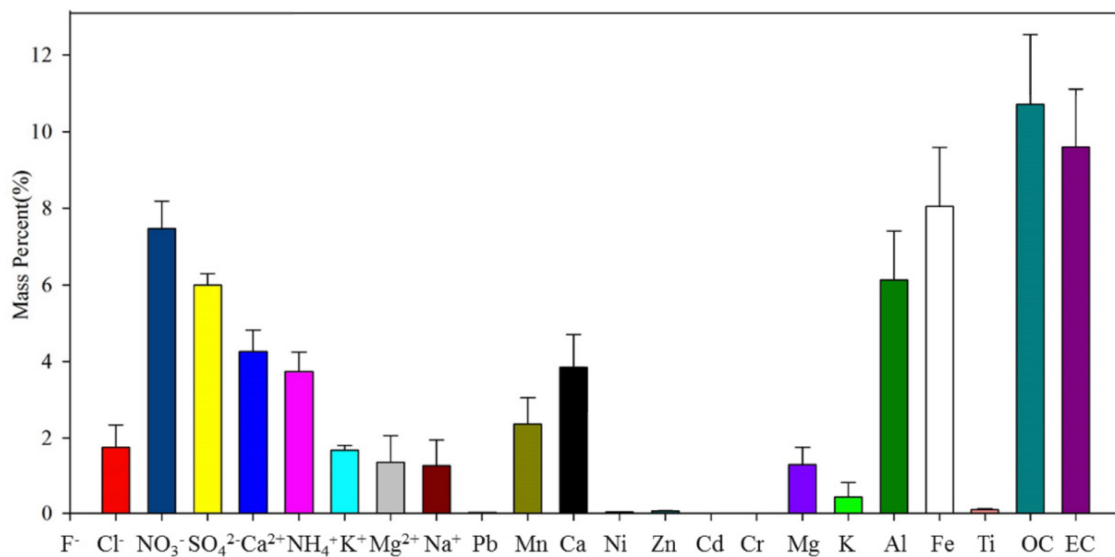


**Fig. 8.** Chemical constituents of PM<sub>10</sub> collected from the alluvial soils located in the middle regions of the Kaoping River.

Following by the carbonaceous species in alluvium soils, WSIs ranked the second, including major cations of Ca<sup>2+</sup>, Na<sup>+</sup>, Mg<sup>2+</sup>, and K<sup>+</sup>, and the major anions of NO<sub>3</sub><sup>-</sup>, SO<sub>4</sub><sup>2-</sup>, and Cl<sup>-</sup>. Among the water-soluble cations, Ca<sup>2+</sup> was the richest cation, with a mass percentage of 4.25 ± 0.57%, while NO<sub>3</sub><sup>-</sup> was the most abundant anion, with a mass percentage of 7.46 ± 0.72%, which could be related to intense agricultural activities (i.e., the swine industrial, dairy, and fertilizing processing) on both banks of the Kaoping River (Viana *et al.*, 2006; Han *et al.*, 2007). The variance of WSIs, including Cl<sup>-</sup>, NO<sub>3</sub><sup>-</sup>, SO<sub>4</sub><sup>2-</sup>, Na<sup>+</sup>, NH<sub>4</sub><sup>+</sup>, and Mg<sup>2+</sup>, were markedly higher than those of trace metallic elements. It suggested that the constituent of the fluvial basin of the Kaoping River transported toward downstream areas probably contained various types of anthropogenic pollutants.

Additionally, previous studies have reported that Fe, Al, or Ca are the most abundant crustal metals of the aeolian dust at the background sites (Taiwan EPA, 2009; Kuo *et al.*, 2010; Kong *et al.*, 2011). In the present study, the dominant metallic contents of the aeolian dust in the Kaoping River were crustal materials (Fe, Al, and Ca) which were similar to those of the aeolian dust sampled from rivers in central Taiwan (Taiwan EPA, 2009; Kuo *et al.*, 2010; Chen *et al.*, 2015). For the contents of Fe, Al, or Ca in the alluvium soils, no significant variance ( $p > 0.05$ ) was observed among the five sampling sites as shown in Table 2. These results indicated that the chemical characteristics of alluvial soils were highly similar and evenly distributed from the downstream to the upstream of the Kaoping River, suggesting that they might be originated from same mother rocks.

#### Indicators of ADE Determined by Metallic Elements

Metallic elements in size-segregated particulate matters were generally discussed and their elemental ratios could determine the contribution of trans-boundary or local air pollutants at the studied sites (Tang *et al.*, 2006; Kuo *et al.*, 2010; Chen *et al.*, 2015; Li *et al.*, 2015; Taniguchi *et al.*, 2016). Taiwan EPA (2009) has reported that the fluvial

basin of major rivers in central Taiwan was rich in crustal elements (e.g., Fe, Al, and Ca) and the mass ratio of some crustal elements to reference elements could be identified as valuable indicators describing the influences of ADEs on the ambient particulate matters. Thus, this study attempts to discuss the relations between elemental ratios and aeolian dust in different sampling periods.

To distinguish the features of the ADEs in different periods along the Kaoping River Valley, a comparison of mass ratios of gross crustal elements ( $\sum$ CEs) to the gross anthropogenic elements ( $\sum$ AEs) for the PM<sub>10</sub> samples during the ADE periods is presented in Table 3. The mass ratios of  $\sum$ CEs to  $\sum$ AEs ( $\sum$ CEs/ $\sum$ AEs) in the Stage I of the ADE were 2.5- to 3.9-fold higher than those on regular days and in the Stage II of the ADE, indicating the influence of aeolian dust could apparently increase the portion of crustal elements in ambient PM<sub>10</sub> in the Stage II of the ADE. The portion of crustal elements in particulate matters apparently increases due to the influence of ADEs correspondingly (Chen *et al.*, 2015; Taniguchi *et al.*, 2016). Therefore, this study further determined representative indicators for ascertaining ADEs by the mass ratios of crustal elements (i.e., Fe, Al, and Ca) to reference elements (trace elements). Among different arrangements in the mass ratios of crustal elements to anthropogenic elements, the mass ratios of Fe/Cd (211.6–3,957.2) were markedly higher than those of Al/Cd (1,114.0–3,746.3) in the Stage I of the ADE. These findings supported the results obtained from this study that higher mass ratios of Fe/Cd and Al/Cd in the Stage I of the ADE were highly correlated with the occurrence of aeolian dust (Taiwan EPA, 2009).

Regarding the aforementioned chemical fingerprints of alluvial soils, Fe was the specific metallic element of PM<sub>10</sub> in the influential areas, which can be treated as an representative crustal element in the present study due to its high content in the aeolian dust and no significant variance ( $p > 0.05$ ) of alluvial soils along the Kaoping River. The extremely low content of Cd was observed in the fluvial

**Table 2.** Metallic content of alluvium soils collected on bare lands along the Kaoping River.

Metals \ Locations	Site 1 (n = 6)	Site 2 (n = 6)	Site 3 (n = 6)	Site 4 (n = 6)	Site 5 (n = 6)	p values
<b>Pb</b>	30.7 ± 8.05	28.3 ± 14.15	39.2 ± 18.1	26.15 ± 6.85	25.88 ± 14.91	0.721
Mn	506.4 ± 77.1	338.9 ± 109.6	365.8 ± 80.1	560.2 ± 73.4	223.5 ± 41.1	0.001
Al	4346 ± 356	3945.4 ± 465.9	4105.6 ± 227.8	3698.4 ± 272.8	3567.1 ± 240.9	0.885
Ni	37.5 ± 14.0	39.2 ± 13.81	20.6 ± 9.6	33.9 ± 10.2	39.2 ± 13.8	0.528
Zn	47.6 ± 26.9	70.4 ± 15.6	47.5 ± 28.1	69.3 ± 43.8	33.9 ± 6.7	0.439
Cd	0.28 ± 0.24	0.38 ± 0.17	0.22 ± 0.13	0.27 ± 0.17	0.15 ± 0.02	0.544
Cr	1.7 ± 1.08	1.98 ± 0.96	1.02 ± 0.4	1.55 ± 0.71	4.23 ± 3.03	0.601
Mg	326.6 ± 80.9	248.7 ± 67.3	185.2 ± 44.4	386.2 ± 105.8	416.8 ± 113.7	0.027
K	363.6 ± 173	488.3 ± 202.8	607.5 ± 115.7	578.4 ± 318.4	681.2 ± 124.5	0.388
Ca	1720 ± 528	1646.2 ± 203.6	2136.6 ± 247.2	2255.0 ± 248.2	1299.4 ± 217.6	0.925
Fe	6546 ± 394.5	5844.7 ± 206.2	5276.7 ± 500.9	7650.1 ± 2330.0	6664.6 ± 284.9	0.204
As	11.07 ± 3.55	12.01 ± 3.07	13.53 ± 2.72	16.72 ± 5.61	9.95 ± 1.53	0.221
Ti	42.11 ± 16.71	37.55 ± 4.64	43.75 ± 9.95	35.5 ± 13.21	34.74 ± 14.87	0.872

<sup>a</sup> Unit:  $\mu\text{g g}^{-1}$ .<sup>b</sup> n: numbers of measurements; SD: standard deviation.**Table 3.** Mass ratios of crustal elements to reference elements for PM<sub>10</sub> sampled along the Kaoping River on regular days and in the periods during and after the ADE.

Sites	KA			KB			PC			PD		
	Stages	RD	1 <sup>st</sup>	2 <sup>nd</sup>	RD	1 <sup>st</sup>	2 <sup>nd</sup>	RD	1 <sup>st</sup>	2 <sup>nd</sup>	RD	1 <sup>st</sup>
$\sum\text{CEs}/\sum\text{AEs}$	2.24	6.39	3.64	1.61	6.20	3.43	2.04	5.01	4.06	2.17	5.52	2.72
Fe/Cd	190.5	3957.2	129.3	115.5	3831.6	103.7	194.4	829.8	94.1	211.6	1330.3	122.1
Al/Cd	69.7	3746.3	146.5	30.7	2495.5	130.7	68.5	1114.0	61.1	78.6	1464.3	70.4

<sup>a</sup> RD: Regular days.<sup>b</sup> 1<sup>st</sup>: During the ADE.<sup>c</sup> 2<sup>nd</sup>: After the ADE.<sup>d</sup>  $\sum\text{CEs}/\sum\text{AEs}$ : mass ratio of gross crustal elements and gross anthropogenic elements.

soils, as shown in Table 2, and there was no significant variance ( $p > 0.05$ ) of Cd through nonparametric statistics among the five sampling sites along the Kaoping River. These results implied that Cd in alluvial soils evenly existed along the Kaoping River surroundings, and its lowest concentration of metallic elements was appropriate to be recognized as a background level. Accordingly, the present study selected Cd as a reference anthropogenic element under consideration of all trace elements analyzed. Consequently, this study revealed that the mass ratio of Fe/Cd could be recognized as an effective indicator for verifying the occurrence of ADEs in the Kaoping River Valley (Tang *et al.*, 2006; Taiwan EPA, 2009; Kuo *et al.*, 2010).

#### Source Apportionment of PM<sub>10</sub> on Regular Days and during and after the ADE

Source identification is thought as one of the key components for improving deteriorative air quality. Many source apportionment studies have attempted to develop and implement air pollution control strategies for urban areas (Li *et al.*, 2013a; Ni *et al.*, 2013; Taiwo *et al.*, 2016). Receptor models have been widely used to estimate the contribution from various types of sources, except for aeolian dust, to ambient air quality. The principles of mass conservation for the chemical mass balance (CMB) receptor model are applied to identify and apportion the sources of

airborne particles. The CMB receptor model uses an effective variance least-square procedure to apportion the ambient airborne particles to selected sources.

In the present study, USEPA-CMB 8.0 Model (Lioulter, 2004) was applied for conducting the source apportionment of ambient PM<sub>10</sub> sampled at four sites along the Kaoping River. The source apportionment results of ambient PM<sub>10</sub> sampled on regular days and in the periods during and after the ADE are summarized in Table 4. It shows an obvious spatiotemporal distribution of PM<sub>10</sub> sources in different sampling periods. The resolved sources of PM<sub>10</sub> ranked in the order of aeolian dust (12.9%–33.1%) > secondary sulfate (12.2%–14.9%) > sea salts (10.4%–13.5%) > vehicular exhaust (7.2%–10.5%) > road dust (3.2%–10.5%) > secondary nitrate (6.5%–9.9%) > steel industries (2.7%–8.5%) > OC (3.6%–5.8%) > EC (2.2%–4.3%) > petrochemical industries (2.1%–5.2%) during the ADE (Stage I). Based on the source apportionment results, PM<sub>10</sub> sources can be further divided into four different types of sources, including natural sources, anthropogenic sources, vehicular exhausts, and secondary sources.

The high percentages of natural sources were found at the sampling sites, suggesting that aeolian dust and sea salts were the major sources during and after the ADE since typhoon outflow circulation deduced prevailing winds from Bashi Channel to the Kaoping River Valley. Thus,

**Table 4.** Source apportionment of PM<sub>10</sub> on regular days and in the periods during (stage I) and after (stage II) the ADE.

Emission Sources	Regular Days				Stage I				Stage II			
	KA	KB	PC	PD <sup>#</sup>	KA 1 <sup>st</sup>	KB 1 <sup>st</sup>	PC 1 <sup>st</sup>	PD 1 <sup>st</sup>	KA 2 <sup>nd</sup>	KB 2 <sup>nd</sup>	PC 2 <sup>nd</sup>	PD 2 <sup>nd</sup>
Sea Salts	8.43	6.72	4.14	4.29	12.8	10.4	10.6	13.5	10.9	7.8	7.4	
Petrochemical Industries	9.2	12.6	4.6	9.5	2.1	5.2	3.2	2.5	8.4	10.2	5.5	11.6
Steel Industries	8.2	8.2	10.8	11.7	5.5	7.2	2.7	4.7	9.5	8.5	6.8	9.1
Secondary Nitrate	7.9	11.1	9.9	10.5	7.2	6.5	9.9	8.5	8.4	7.3	6.1	12.5
Organic Carbon	6.7	5.3	6.4	7.3	4.6	3.6	4.3	5.8	4.7	3.7	6.2	6.5
Element Carbon	1.8	3.1	3.6	4.2	2.5	2.2	3.2	2.3	2.5	3.3	4.3	5.2
Biomass Burning	5.5	3.7	10.5	11.3	1.5	0.9	0.8	1.5	1.5	1.7	3.6	3.1
Vehicular Exhausts	7.1	6.6	10.4	10.8	7.8	7.2	9.8	10.5	9.7	10.3	16.5	12.2
Aeolian Dust	6.17	2.68	1.01	2.66	33.1	28.1	12.9	24.1	20.5	17.8	12.3	14.3
Secondary Sulfate	9.8	11.2	10.7	10.1	12.2	13.5	14.9	12.2	13.7	11.9	9.3	11.0
Incinerators	3.9	3.7	1.3	2.5	1.3	1.6	-	1.1	1.2	1.7	-	-
Road Dust	7.8	6.3	10.4	5.8	4.5	3.2	10.5	2.1	3.7	3.9	8.1	3.2
Undetermined	17.5	18.8	16.2	9.4	4.9	10.4	17.2	11.2	5.9	8.8	13.5	15.5
Mass Percentage (%)	82.5	81.2	83.8	90.6	95.1	89.6	82.8	88.8	94.1	91.2	86.5	84.5
R <sup>2</sup>	0.99	0.99	0.99	0.99	0.99	1.00	1.00	1.00	1.00	1.00	0.99	1.00

<sup>a,c</sup>“ emission source that is not apportioned.

<sup>b</sup> Units: % (exclude R<sup>2</sup>).

the aeolian dust was attributed not only from the alluvium soils on bare lands but also from oceanic spray during the ADE. Aeolian dust and sea salts commonly regarded as two typical natural sources in southern Taiwan, contributing to 1.01–6.17% and 4.14–8.43% of ambient PM<sub>10</sub>, respectively, on regular days. During the ADE (Stage I), the contribution of natural sources increased significantly which thus highly influenced the particulate air quality on both sides of the Kaoping River. However, as the wind speeds decreased gradually after the ADE, the mass percentages of aeolian dust and sea salts reduced correspondingly. Nevertheless, aeolian dust contributed to 17.8–20.5% of PM<sub>10</sub> on the right bank and 12.3–14.3% on the left bank of the Kaoping River after the ADE (Stage II). The results indicated that a small amount of finer aeolian dust emitted from the bare lands could be still suspended in the ambient air during the period of Stage II (Lin *et al.*, 2007; Kuo *et al.*, 2010; Taiwo *et al.*, 2016). Additionally, the mass percentages of sea salts obtained from sites KA and PD were always higher than other sites during the ADE. Additionally, the content of sea salts decreased with distance from the estuary to the inland of the Kaoping River (Tsai *et al.*, 2010).

Some anthropogenic sources (i.e., petrochemical plants and steel plants) were located nearby the Kaoping River in southern Taiwan. During the ADE (Stage I), strong winds blew southwesterly from the estuary of the Kaoping River resulted in relatively higher percentages of natural sources than those on regular days and after the ADE. The steel industries located in the Xiaogang District, comprising the largest iron works and steel manufacturing complex in Taiwan, can influence the ambient particulate air quality along the Kaoping River on regular days through sea-land breezes (Tsai *et al.*, 2007; Tsai *et al.*, 2008, 2010). The percentages of vehicular exhaust and road dust contributed to PM<sub>10</sub> during the ADE (Stage I) were lower than those on regular days and after the ADE (Stage II). Moreover, secondary inorganic aerosols (i.e., secondary sulfate and nitrate) in different sampling periods were in the order of regular days > after the ADE (Stage II) > during the ADE (Stage I). More aged particles possibly derived from industrial complexes at the both sides of the downstream region of the Kaoping River due to photochemical reactions and then transporting to the studied area on regular days.

## CONCLUSIONS

The present study first investigated the influences of aeolian dust driving by subtropical typhoon circulation outflow on ambient particulate air quality in southern Taiwan. The chemical characteristics and spatiotemporal distribution of PM<sub>10</sub> along the Kaoping River Valley were thoroughly discussed on regular days and in the periods during and after the ADE. Unpredictable ADE drastically increased the PM<sub>10</sub> concentrations to 21.2- to 27.2-fold higher than those on regular days and could quickly reach the maximum PM<sub>10</sub> concentrations within two hours while Typhoon Doksuri approached the Bashi Channel on June 29–30, 2012.

Compared with several indicators, including the mass

ratios of Fe/Cd and OC/EC, and the molar ratios of  $[Cl^-]/[Na^+]$  in  $PM_{10}$  both on regular days and during the ADE (Stage I), we found that these indicators varied apparently with the ADE and were highly influenced by Typhoon Dokuri. These indicators will be valuable and potentially applicable for warning the residents lived nearby the Kaoping River Valley, which can be further used to verify the occurrence of ADE during the typhoon season. Under the effects of strong winds exerted by typhoon outflow circulations, air flow accompanied by a substantial amount of SSPs resulted in high molar ratios of  $[Cl^-]/[Na^+]$  and a lower  $Cl^-$  deficit for the aeolian dust. In addition, the highest content of Fe and the lowest content of Cd in alluvial soils were appropriate to be recognized as represented elements, respectively. The mass ratio of Fe to Cd could be acknowledged as an indicator for identifying ADEs in future studies. The average mass ratios of OC and EC (OC/EC) ranged from 1.18 to 1.53 during the ADE, indicating that strong winds were not favorable for forming secondary organic aerosols (SOAs). As a result, the aeolian dust emitted from the bare lands were the dominant component in  $PM_{10}$ . These findings led to a better understanding of aerosol climatology during the ADE. The mass ratios of Fe/Cd increased significantly during the ADE, which was much higher than other metallic ratios, suggesting that Fe/Cd could be another indicator for verifying the ADE.

Combining SSPs reconstruction with CMB receptor modeling revealed that aeolian dust and SSPs were the major components of  $PM_{10}$  during the ADE investigated in the present study. The contributions of aeolian dust emitted from the bare lands to  $PM_{10}$  were in the range of 43.1%–51.1% on the right bank and 19.9%–22.1% on the left bank of the Kaoping River. Moreover, WRF model can effectively describe hourly wind field based on the landscape of the studied region, while SURFER spatial plotting software can show the variation of particulate matter concentrations locating the hot spots influenced by aeolian dust. Intergrading WRF model and SURFER spatial plotting software, this study successfully verified the hot spots at the downstream of the Kaoping River during the ADE where aeolian dust was originally blown from the alluvial soils on the estuary of the Kaoping River.

## ACKNOWLEDGMENTS

This study was performed under the auspices of Pingtung Environmental Protection Bureau and Arounding-You Environmental Engineering Consultants Co. Ltd. The authors would also like to express their sincere appreciation to the Kaoping River Weir Management Center, the Fo-Guang-Shan Buddha Memorial Museum, the Yutian Elementary School, and the Sui-Branch of Huei-Nung Elementary School for providing constant assistances in the field sampling of  $PM_{10}$  in this study.

## SUPPLEMENTARY MATERIAL

Supplementary data associated with this article can be found in the online version at <http://www.aaqr.org>.

## REFERENCES

- Brook, J.R., Poirot, R.L., Dann, T.F., Lee, P.K., Lillyman, C.D. and Ip, T. (2007). Assessing sources of  $PM_{2.5}$  in cities influenced by regional transport. *J. Toxicol. Environ. Health Part A* 70: 191–199.
- Bryant, R.G., Bigg, G.R., Mahowald, N.M., Eckardt, F.D. and Ross, S.G. (2007). Dust emission response to climate in southern Africa. *J. Geophys. Res.* 112: D09207.
- Cao, J.J., Lee, S.C., Ho, K.F., Zhang, X.Y., Zou, S.C., Fung, K., Chow, J.C. and Watson, J.G. (2003). Characteristics of carbonaceous aerosol in Pearl River Delta Region, China during 2001 winter period. *Atmos. Environ.* 37: 1451–1460.
- Cao, J.J., Shen, Z., Chow, J.C., Qi, G. and Watson, J.G. (2009). Seasonal variations and sources of mass and chemical composition for  $PM_{10}$  aerosol in Hangzhou, China. *Particuology* 7: 161–168.
- Chang, C.T., Chang, Y.M., Lin, W.Y. and Wu, M.C. (2011). Fugitive dust emission source profiles and assessment of selected control strategies for particulate matter at gravel processing sites in Taiwan. *J. Air Waste Manage. Assoc.* 60: 1262–1268.
- Chen, Y.C., Hsu, C.Y., Lin, S.L., Chang-Chien, G.U., Chen, M.J., Fang, G.C. and Chiang, H.C. (2015). Characteristics of concentrations and metal compositions for  $PM_{2.5}$  and  $PM_{2.5-10}$  in Yunlin County, Taiwan during air quality deterioration. *Aerosol Air Qual. Res.* 15: 2571–2583.
- Chester, R., Nimmo, M., Keyse, S. and Zhang, Z. (2000). Trace metal chemistry of particulate aerosols from the UK mainland coastal rim of the NE Irish Sea. *Atmos. Environ.* 34: 949–958.
- Chow, J.C. (1995). Measurement methods to determine compliance with ambient air quality standards for suspended particles. *J. Air Waste Manage. Assoc.* 45: 320–382.
- Chow, J.C., Watson, J.G., Green, M.C., Lowenthal, D.H., Bates, B., Oslund, W. and Torres, G. (2000). Cross-border transport and spatial variability of suspended particles in Mexicali and California's Imperial Valley. *Atmos. Environ.* 34: 1833–1843.
- Colbeck, I. and Harrison, R.M. (1984). Ozone-secondary aerosol visibility relationships in northwest England. *Sci. Total Environ.* 34: 87–100.
- Eckardt, F.D. and Kuring, N. (2005). SeaWiFS identifies dust sources in the Namib Desert. *Int. J. Remote Sens.* 26: 4159–4167.
- Engelbrecht, J.P. and Jayanty, R.K.M. (2013). Assessing sources of airborne mineral dust and other aerosols, in Iraq. *Aeolian Res.* 9: 153–160.
- Han, L., Zhuang, G., Cheng, S. and Li, J. (2007). Elemental carbon in urban soils and road dust in Xi'an, China and its implication for air pollution. *Atmos. Environ.* 41: 7533–7546.
- Hopke, P.K., Ito, K., Mar, T., Christensen, W.F., Eatough, D.J. and Henry, R.C. (2006). PM source apportionment and health effects: 1. Inter-comparison of source apportionment results. *J. Exposure Sci. Environ.*

- Epidemiol.* 16: 275–286.
- Kong, S., Ji, Y., Lu, B., Chen, L., Han, B., Li, Z. and Bai, Z. (2011). Characterization of PM<sub>10</sub> source profiles for fugitive dust in Fushun-A city famous for coal. *Atmos. Environ.* 45: 5351–5365.
- Kumar, A., Sarin, M.M. and Sudheer, A.K. (2008). Mineral and anthropogenic aerosols in Arabian Sea-atmospheric boundary layer: Sources and spatial variability. *Atmos. Environ.* 42: 5169–5181.
- Kumar, A., Sudheer, A.K., Goswami, V. and Bhushan, R. (2012). Influence of continental outflow on aerosol chemical characteristics over the Arabian Sea during winter. *Atmos. Environ.* 50: 182–191.
- Kuo, C.Y., Wang, J.Y., Chang, S.H. and Chen, M.C. (2010). Study of metal concentrations on the environment near diesel transport routes. *Atmos. Environ.* 43: 3070–3076.
- Lavanchy, V.M.H., Gaggeler, H.W., Nyeki, S. and Baltensperger, U. (1999). Elemental carbon (EC) and black carbon (BC) measurements with a thermal method and an aethalometer at the high-alpine research station Jungfraujoch. *Atmos. Environ.* 33: 2759–2769.
- Li, T.C., Chen, W.H., Yuan, C.S., Wu, S.P. and Wang, X.H. (2013a). Physicochemical characteristics and source apportionment of atmospheric particles in Kinmen-Xiamen Airshed. *Aerosol Air Qual. Res.* 13: 308–323.
- Li, T.C., Chen, W.H., Yuan, C.S., Wu, S.P. and Wang, X.H. (2013b). Diurnal variation and chemical characteristics of atmospheric aerosol particles and their source fingerprints at Xiamen Bay. *Aerosol Air Qual. Res.* 13: 596–607.
- Li, T.C., Yuan, C.S., Lo, K.C., Hung, C.H., Wu, S.P. and Tong, C. (2015). Seasonal variation and chemical characteristics of atmospheric particles at three islands in the Taiwan Strait. *Aerosol Air Qual. Res.* 15: 2277–2290.
- Lin, C.W. and Yeh, J.F. (2007). Estimating dust emission from a sandbank on the downstream Jhuoshuei River under strong wind conditions. *Atmos. Environ.* 41: 4553–7561.
- Meng, Z. and Lu, B. (2007). Dust events as a risk factor for daily hospitalization for respiratory and cardiovascular diseases in Minqin, China. *Atmos. Environ.* 41: 7048–7058.
- Mkoma, S.L., Maenhaut, W., Chi, X., Wang, W. and Raes, N. (2009). Characterization of PM<sub>10</sub> atmospheric aerosols for the wet season 2005 at two sites in East Africa. *Atmos. Environ.* 43: 631–639.
- Nayebare, S.R., Aburizaiza, O.S., Khwaja, H.A., Siddique, A., Hussain, M.M., Zeb, J.H., Khatib, F., Carpenter, D.O. and Blake, D.R. (2015). Chemical characterization and source apportionment of PM<sub>2.5</sub> in Rabigh, Saudi Arabia. *Aerosol Air Qual. Res.* 16: 3114–3129.
- Ni, T., Li, P., Han, B., Bai, Z., Ding, X., Wang, Q., Huo, J. and Lu, B. (2013). Spatial and temporal variation of chemical composition and mass closure of ambient PM<sub>10</sub> in Tianjin, China. *Aerosol Air Qual. Res.* 13: 1832–1846.
- Sun, K., Liu, H., Ding, A. and Wang, X. (2016). WRF-chem simulation of a severe haze episode in the Yangtze River Delta, China. *Aerosol Air Qual. Res.* 16: 1268–1283.
- Syu, J.Y., Cheng, Y., Kao, Y.Y., Liang, C.S., Yan, Y.L., Lai, C.Y., Chang, C.T., Chen, C.C., Young C.Y., Wu, Y.L. and Lin, W.Y. (2016). The horizontal and vertical characteristics of aeolian dust from riverbed. *Aerosol Air Qual. Res.* 16: 3026–3036.
- Taiwan EPA (2009). Evaluation of the effects of aeolian dust from rivers on the aerosol in central Taiwan, Taiwan.
- Taiwan WRA (2009). Deflation prevention strategy analysis on exposed sand beach from Lilin Bridge to the river mouth of Kaoping River, Taiwan.
- Taiwo, A.M. (2016). Source apportionment of urban background particulate matter in Birmingham, United Kingdom using a mass closure model. *Aerosol Air Qual. Res.* 16: 1244–1252.
- Tang, Y. and Han, G.L. (2006). Characteristics of major elements and heavy metals in atmospheric dust in Beijing, China. *J. Geochem. Explor.* 176: 114–119.
- Taniguchi, Y., Shimada, K., Takami, A., Lin, N.H., Chak, K., Chan, C.K., Kim, Y.P. and Hatakeyama, S. (2017). Transboundary and local air pollutants in western Japan distinguished on the basis of ratios of metallic elements in size-segregated aerosols. *Aerosol Air Qual. Res. in Press*.
- Tsai, H.H., Ti, T.H., Yuan, C.S., Hung, C.H. and Lin, C. (2008). Effects of sea-land breezes on the spatial and temporal distribution of gaseous air pollutants around the coastal region of southern Taiwan. *J. Environ. Eng. Manage.* 18: 387–396.
- Tsai, H.H., Yuan, C.S., Hung, C.H. and Lin, Y.C. (2011). Comparing physicochemical properties of ambient particulate matter of hot spots in a highly polluted air quality zone. *Aerosol Air Qual. Res.* 10: 331–344.
- Tsai, J.H., Huang, K.L., Lin, N.H., Chen, S.J., Lin, T.C., Chen, S.C., Lin, C.C., Hsu, S.C. and Lin, W.Y. (2012). Influence of an Asian dust storm and southeast Asian biomass burning on the characteristics of seashore atmospheric aerosols in southern Taiwan. *Aerosol Air Qual. Res.* 12: 1105–1115.
- Tsai, Y.I. and Chen, C.L. (2006). Characterization of Asian dust storm and non-Asian dust storm PM<sub>2.5</sub> aerosol in southern Taiwan. *Atmos. Environ.* 40: 4734–4750.
- Wang, J., Li, X., Zhang, W., Jiang, N., Zhang, R. and Tang, X. (2016). Secondary PM<sub>2.5</sub> in Zhengzhou, China: Chemical species based on three years of observations. *Aerosol Air Qual. Res.* 16: 91–104.
- Wang, X.L., Chow, J.C., Kohl, S.D., Yatavelli, L.N.R., Percy, K.E., Legge, A.H. and Watson, J.G. (2015). Wind erosion potential for fugitive dust sources in the Athabasca oil sands region. *Aeolian Res.* 18: 121–134.
- Xu, Y., Sun, Q.Q., Yi, L., Wang, A., Li, Y.H. and Chen, J. (2014). The source of natural and anthropogenic heavy metals in the sediments of the Minjiang River Estuary (SE China): Implications for historical pollution. *Sci. Total Environ.* 493: 729–736.
- Yuan, C.S., Hai, C.X. and Zhao, M. (2006). Source profiles and fingerprints of fine and coarse sands resuspended from soils sampled in Central Inner Mongolia. *China Particulology* 4: 304–311.
- Zhao, M., Wang, S., Tan, J., Hua, Y., Wu, D. and Hao, J.

(2016). Variation of urban atmospheric ammonia pollution and its relation with PM<sub>2.5</sub> chemical property in Winter of Beijing, China. *Aerosol Air Qual. Res.* 16: 1378–1389.

*Received for review, August 2, 2017*

*Revised, August 23, 2017*

*Accepted, August 23, 2017*